AIAA JOURNAL
Vol. 38, No. 4, April 2000

Technical Notes

TECHNICAL NOTES are short manuscripts describing new developments or important results of a preliminary nature. These Notes cannot exceed 6 manuscript pages and 3 figures; a page of text may be substituted for a figure and vice versa. After informal review by the editors, they may be published within a few months of the date of receipt. Style requirements are the same as for regular contributions (see inside back cover).

Damping Effects in Nonlinear Panel Flutter

Maher N. Bismarck-Nasr* and Carlos Alberto Bones†
Instituto Tecnológico de Aeronáutica,
12228-900 São José dos Campos, Brazil

I. Introduction

AEROELASTICITY of plates and shells constitutes an important aspect in the design of high-speed vehicles. Several reviews and survey papers[1–5] relate the extensive analytical and experimental research that has been achieved on the subject during the past few decades. Since the earlier works on panel flutter, the nonlinear structural problem has been adressed by several investigators using the Galerkin formulation. For the solution of the nonlinear problem, several methods were adopted. Dowell[6] used the direct numerical integration technique, Morino[7] employed the perturbation methods, and the harmonic balance technique was used by Fung.[8] Limit-cycle amplitude panel flutter using the finite element method was studied by Han and Yang[9] and Mei and Wang.[10] In the present work an attempt is made to assess and discuss the effect of damping in nonlinear panel flutter analysis. Structural, viscoelastic, and aerodynamic dampings are included in the formulation, and their effect on the stability boundary of the shell is presented. A finite element formulation is used for the problem formulation, and the nonlinear aeroelastic solution is made using the perturbation method.

II. Problem Formulation

In this section the aeroelastic problem of large deformations of curved panels is considered. For a doubly curved isotropic thin shell panel, using Novozhilov's[11] nonlinear shell theory, neglecting the transverse shear effect and using Kirchhoff's assumption, the midplane strains read[11]

$$\varepsilon_{xx} = \frac{\partial u}{\partial x} - \frac{w}{R_x} + \frac{1}{2}\left(\frac{\partial w}{\partial x}\right)^2 - z\frac{\partial^2 w}{\partial x^2}$$

$$\varepsilon_{yy} = \frac{\partial v}{\partial y} - \frac{w}{R_y} + \frac{1}{2}\left(\frac{\partial w}{\partial y}\right)^2 - z\frac{\partial^2 w}{\partial y^2}$$

$$\varepsilon_{xy} = \frac{1}{2}\left(\frac{\partial u}{\partial y} + \frac{\partial v}{\partial x} - 2z\frac{\partial^2 w}{\partial x\,\partial y}\right) + \frac{1}{2}\frac{\partial w}{\partial x}\frac{\partial w}{\partial y} \qquad (1)$$

where ε_{ij} are the strain tensor components; u, v, and w are the midplane displacement components in the x, y, and z directions; and R_x, R_y are the radius of curvature in the x, y directions. The midplane stress-strain relationships for thin isotropic shell read

$$\sigma_{xx} = \frac{E}{(1-\nu^2)}(\varepsilon_{xx} + \nu\varepsilon_{yy})$$

$$\sigma_{yy} = \frac{E}{(1-\nu^2)}(\varepsilon_{yy} + \nu\varepsilon_{xx}), \qquad \sigma_{xy} = 2G\varepsilon_{xy} \qquad (2)$$

where σ_{ij} are the stress tensor components, E is the Young's modulus, G is the shear modulus, and ν is Poisson's ratio. The strain energy of deformation can be written as

$$U = \frac{1}{2}\int_V (\sigma_{xx}\varepsilon_{xx} + \sigma_{yy}\varepsilon_{yy} + \sigma_{xy}\varepsilon_{xy})\,\mathrm{d}x\,\mathrm{d}y\,\mathrm{d}z = U(u, v, w) \qquad (3)$$

The kinetic energy functional, neglecting the rotary inertias terms for thin shells, reads

$$T = \frac{1}{2}\int_A \rho_m h\left(\frac{\partial u}{\partial t}\right)^2 + \left(\frac{\partial v}{\partial t}\right)^2 + \left(\frac{\partial w}{\partial t}\right)^2 \mathrm{d}A \qquad (4)$$

where ρ is the material density and h is the shell thickness. The work done by the external aerodynamic forces reads[5]

$$W = -\int_A \frac{2Q}{(M^2-1)^{\frac{1}{2}}}\left(\frac{\partial w}{\partial x} + \frac{M^2-2}{V(M^2-1)}\frac{\partial w}{\partial t}\right)w\,\mathrm{d}A \qquad (5)$$

where $Q = \rho_a V^2/2$ is the dynamic freestream pressure, ρ_a is the freestream density, V is the freestream velocity, and M is the freestream Mach number. The sources of damping in aeroelasticity of plates and shells are of aerodynamic and structural nature. The aerodynamic damping enters in the formulation through the term proportional to the velocity in the aerodynamic surface loading expression as given in Eq. (5). This damping is a mass proportional type and always has a stabilizing effect. The structural damping can be formulated through a viscous-type damping proportional to the velocity; again, this type of damping always has a stabilizing effect and will furnish in the finite element formulation a symmetric matrix that is proportional to the mass matrix, and its final effect on the stability of the shell is similar to the aerodynamic damping and is cumulative to it. Another type of structural damping that has been considered in aeroelastic analysis is a hysteric-type damping. This can be incorporated in the analysis by writing a damping force proportional to the elastic forces and in phase with the velocity. The work done by the structural damping dissipative forces can be written as

$$W_D = -\int_A \left(c\frac{\partial w}{\partial t} + \frac{ig}{\omega}F_E\right)w\,\mathrm{d}A \qquad (6)$$

where c is the structural viscous material material constant, g is a structural damping parameter, F_E are the elastic forces, and ω is the modulus of the complex frequency response. The Hamilton's principle for the problem at hand can be written as

$$\int_{t_0}^{t_1} \delta(T-U)\,\mathrm{d}t + \int_{t_0}^{t_1} \delta W\,\mathrm{d}t + \int_{t_0}^{t_1} \delta W_D\,\mathrm{d}t = 0 \qquad (7)$$

A finite element solution for the problem at hand can be performed, using rectangular elements preserving C^1 continuity, as previously given in Refs. 12–14 for the linear analysis. The solution of the

Received 20 February 1999; revision received 21 September 1999; accepted for publication 23 October 1999.

*Professor, Division of Aeronautical Engineering. Member AIAA.
†Postgraduate Student, Division of Aeronautical Engineering.

nonlinear stability problem using the perturbation method has been detailed in Ref. 5 and will not be repeated here.

III. Numerical Results and Conclusions

In this section some of the calculations performed using the present formulation are reported, and the results obtained are discussed. The first example presented is a nonlinear aeroelastic solution of a simply supported plate plate, with aspect ratios $a/b = 1$ and 2. The results of the calculations are given in Fig. 1 and are compared with Dowell's[6] solution. Dowell's solution is a direct numerical integration solution using a six-mode Galerkin method. The present solution is a finite element solution with a mesh of 4×4 elements, coupled with the perturbation method. From these results the observation can be made that good agreement has been obtained. The next series of calculations were performed to study the effect of the incorporation of a conservative damping (aerodynamic or structural viscous damping) in the analysis. The results given in Fig. 2 are for simply supported plates, and those shown in Fig. 3 are for a clamped cylindrically curved shell. From these results the observation can be made that the critical dynamic pressure parameter with aerodynamic damping considered is greater than the critical dynamic pressure parameter when damping is not considered, i.e., this type of damping is always conservative in the stability sense. In the results presented, only aerodynamic damping has been considered, the structural viscous damping effect is equivalent, and the only difference is the value of the proportionality constant. The final results presented are flutter solutions with the incorporation of a structural damping proportional to the elastic forces and in phase with the velocity in the analysis. A typical result is shown in Fig. 4.

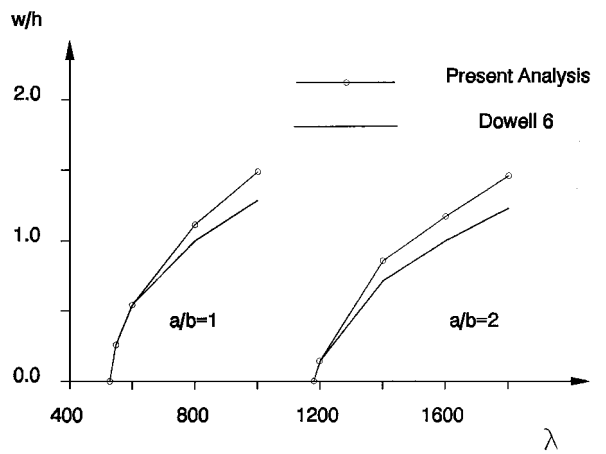

Fig. 1 Nonlinear flutter solution of simply supported flat plates. An aerodynamic damping parameter, $\theta/M = 0.1$, ($\theta = \rho_a a/\rho_m h$), has been used in the calculations.

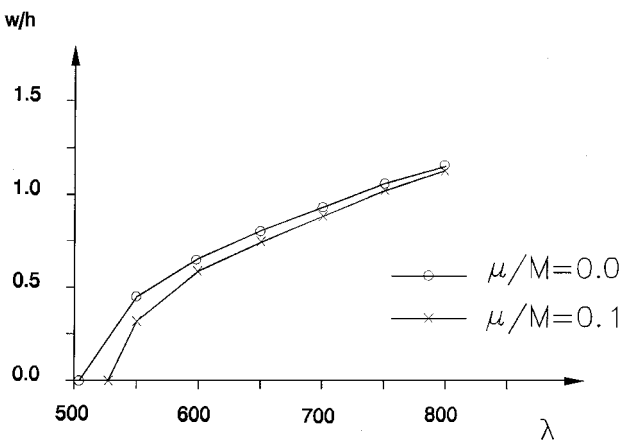

Fig. 2 Effect of the aerodynamic damping in the nonlinear flutter solutions of simply supported square flat plates.

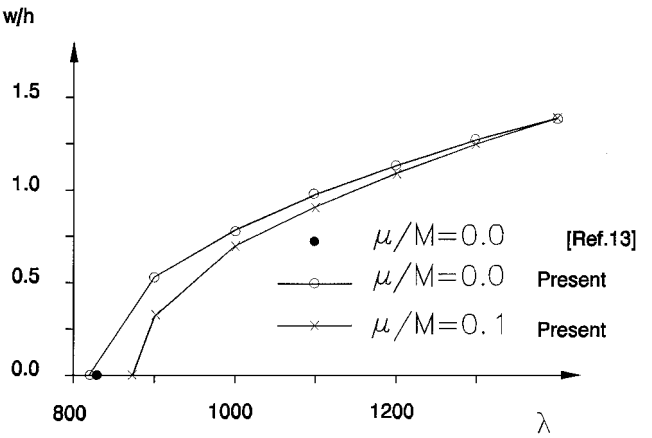

Fig. 3 Effect of the aerodynamic damping in the nonlinear flutter solutions of clamped cylindrically curved shells with rectangular base and flow in the shell axial direction: in the analysis a shell rise parameter $H/h = 2$ has been used. H is the maximum shell rise.

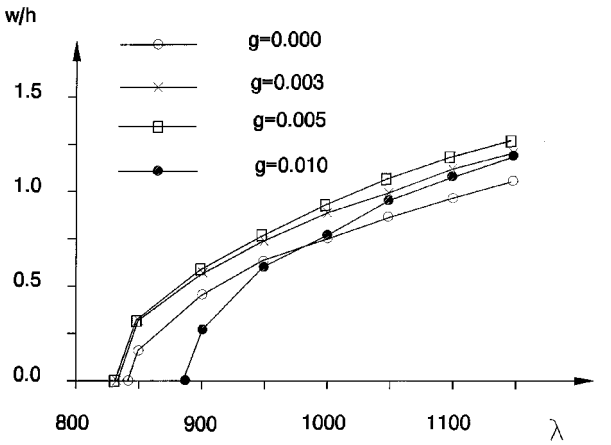

Fig. 4 Effect of the hysteric-type structural damping damping in the nonlinear flutter solutions of clamped square flat plates.

This figure represents the results for a clamped square flat plate in the presence of an aerodynamic damping $\mu/M = 0.1$ and for several hysteric-type structural damping parameters g. From the results obtained, the observation can be made that depending on the value of g used in the analysis this type of damping can stabilize or destabilize the structure. The calculations were repeated (not shown in the figure) for the same configuration and the aerodynamic damping neglected. The destabilizing and stabilizing effect of g on the results shows the same trend and was accentuated. Further calculations were performed with an aerodynamic damping $\mu/M = 0.12$, and the results showed a stabilizing effect with the increase of g. These same conclusions were observed for cylindrically and spherically curved shells and other boundary conditions. The conclusion is when such damping (hysteric-type structural damping) is considered alone (and therefore its presence must be supported with experimental evidences) it can be stabilizing or destabilizing depending on the way of interaction with the structure, i.e., if it dissipates or supplies energy to the system.

Acknowledgment

Grant 300954/91-3 of the Conselho Nacional de desenvolvímento Científico e Tecnológico of Brazil conceded to the first author during the preparation of this work is gratefully acknowledged.

References

[1] Fung, Y. C., *A Summary of the Theories and Experiments on Panel Flutter*, Manual on Aeroelasticity, Pt. 3, AGARD, 1961, Chap. 7.

[2] Johns, D. J., "A Survey of Panel Flutter," Advisory Rept. 1, AGARD, Nov. 1965.

[3]Dowell, E. H., "Panel Flutter: A Review of the Aeroelastic Stability of Plates and Shells," *AIAA Journal*, Vol. 8, No. 3, 1970, pp. 385–399.
[4]Bismarck-Nasr, M. N., "Finite Element Analysis of Aeroelasticity of Plates and Shells," *Applied Mechanics Reviews*, Vol. 45, No. 12, Pt. 1, 1992, pp. 461–482.
[5]Bismarck-Nasr, M. N., "Finite Elements in Aeroelasticity of Plates and Shells," *Applied Mechanics Reviews*, Vol. 49, No. 10, Pt. 2, 1996, pp. S17–S24.
[6]Dowell, E. H., "Nonlinear Oscillations of a Fluttering Plate II," *AIAA Journal*, Vol. 5, No. 10, 1967, pp. 1856–1862.
[7]Morino, L., "A Perturbation Method for Treating Nonlinear Panel Flutter Problems," *AIAA Journal*, Vol. 7, No. 3, 1969, pp. 405–411.
[8]Fung, Y. C., "Two-Dimensional Panel Flutter," *Journal of the Aerospace Sciences*, Vol. 25, No. 3, 1958, pp. 145–159.
[9]Han, A. D., and Yang, T. Y., "Nonlinear Panel Flutter Using High Order Triangular Finite Elements," *AIAA Journal*, Vol. 21, No. 10, 1983, pp. 1453–1461.
[10]Mei, C., and Wang, H. C., "Finite Elements Analysis of Large Amplitude Supersonic Flutter of Panels," *Proceedings of the International Conference on Finite Element Methods*, Gordon and Breach, New York, 1982, pp. 944–951.
[11]Novozhilov, V. V., *Foundations of the Nonlinear Theory of Elasticity*, Graylock Press, Rochester, NY, 1953.
[12]Bismarck-Nasr, M. N., "Analysis of Cylindrically Curved Panels Based on a Two Field Variable Variational Principle," *Applied Mechanics Reviews*, Vol. 46, No. 11, Pt. 2, 1993, pp. 571–578.
[13]Bismarck-Nasr, M. N., "Supersonic Panel Flutter Analysis of Shallow Shells," *AIAA Journal*, Vol. 31, No. 7, 1993, pp. 1349–1351.
[14]Bismarck-Nasr, M. N., *Structural Dynamics in Aeronautical Engineering*, AIAA Education Series, AIAA, Reston, VA, 1999.

A. M. Baz
Associate Editor

Compact Schemes with Spatial Filtering in Computational Aeroacoustics

E. K. Koutsavdis,* G. A. Blaisdell,† and A. S. Lyrintzis‡
Purdue University, West Lafayette, Indiana 47907-1282

Introduction

COMPUTATIONAL aeroacoustics (CAA) is concerned with the accurate prediction of small-amplitude acoustic fluctuations and their correct propagation to the far field. In that respect, CAA poses significant challenges for researchers in that the computational scheme should have high accuracy, good spectral resolution, and low dispersion and diffusion errors. Several schemes have been used to satisfy these criteria. An overview of them can be found in Ref. 1. However, two schemes have appeared to capture significant attention lately. Tam and Webb's[2] dispersion relation preserving scheme, which is based on the minimization of the integrated phase errors in the wave number domain, is one such effort. The scheme, explicit in nature, has proven to be a good solution tool. On the other hand, Lele[3] developed a family of high-order spatially implicit schemes, the compact schemes, a subset of which is the well-known Padé approximations. These schemes, which have been used in CAA in the past, have shown that they require few points per wavelength, which results in lower computational requirements. Furthermore, compact schemes resolve well a large portion of the wave number spectrum.

Received 5 November 1998; revision received 12 July 1999; accepted for publication 20 July 1999.

*Graduate Research Assistant, School of Aeronautics and Astronautics. Student Member AIAA.
†Associate Professor, School of Aeronautics and Astronautics. Senior Member AIAA.
‡Associate Professor, School of Aeronautics and Astronautics. Associate Fellow AIAA.

Besides the stringent requirements on the numerical scheme that were mentioned in the preceding paragraph, the accurate and robust calculation of sound depends heavily on the elimination of any sound waves that could result from reflections of the computed sound waves from the computational boundaries. Many researchers have developed nonreflecting or absorbing boundary conditions for CAA. These boundary conditions should allow both the acoustic fluctuations and the hydrodynamic fluctuations to exit the computational domain, without unwanted reflections. Notably Tam and Webb,[2] Thompson,[4] and Giles[5] have developed nonreflecting boundary conditions. A review of the various possible approaches to the problem can be found in Ref. 6.

Because high-order finite difference schemes do not always resolve effectively the high-wave-number range, filters could be introduced to filter out unwanted high-frequency oscillations that may develop. Lele[3] developed a family of seven-point, pentadiagonal compact spatial filters. These filters have been used in large eddy simulations.[7] Visbal and Gaitonde[8] have used a tridiagonal set of these filters as an alternative to artificial dissipation in computational fluid dynamics calculations of unsteady vortical flows. It is indicated in Ref. 8 that filtering is superior to artificial dissipation.

The use of filtering in CAA has been sparse. For example, explicit spatial filtering is used by Hu[9] in conjunction with a seven-point, fourth-order central scheme, with one-sided differences at the boundary, for numerical stabilization and high-frequency wave damping in CAA with the perfectly matched layer boundary conditions. However, the effect of filtering for CAA calculations has not been adequately studied; this is the main objective of the current Note. The filters and the filtering strategies developed in Ref. 8 are used here. We discuss the savings in CPU time that can be achieved with the use of spatial filtering, as opposed to using higher grid resolutions. A more detailed version of our work can be found in Ref. 10.

Numerical Techniques

A sixth-order compact finite difference scheme[3] with fourth-order-explicit, one-sided finite differences at the boundaries is used. A standard fourth-order Runge–Kutta scheme is used for time advancement. This scheme is coupled with an eighth-order compact filter.[8] Furthermore, Tam and Webb's[2] nonreflecting boundary conditions are used.

One- and two-dimensional linearized Euler equations (LEE) and Euler equation solvers based on the techniques mentioned earlier were developed. Benchmark CAA cases[1] were chosen.

Results and Discussion

LEE Results

Because of space limitations, only two-dimensional results are shown here. For the LEE equations, an initial value problem (Ref. 1, Category III) was chosen. This test case consists of a combination of acoustic, entropy, and vorticity pulses on a freestream of Mach number $M_x = 0.5$ in the positive x direction. The results compared well with the analytical solution for a 200×200 uniform mesh and a time step $\Delta t = 0.125$, with no spatial filtering.[10] A calculation on a coarser grid, 120×120, is shown here to demonstrate the effects of filtering. Higher resolution is required for the useful prediction of the propagation of the acoustic waves. At $t = 75$ the right-going acoustic wave has exited the right boundary because it propagates with a speed $c(M_x + 1)$. The left-going wave, propagating with speed $c(M_x - 1)$, has not exited the left boundary. Oscillations emanating from the boundary as a combined result of a low-order boundary closure and the coarseness of the grid travel upstream (Fig. 1). These oscillations, called q waves,[11] then reflect from the left boundary and grow in amplitude, corrupting the solution with high-frequency components. The use of spatial filtering produces significantly improved results. There is a slight reduction (about 1.5%) of the peak amplitude, and some oscillations remain. This filtering operation added only an additional 18% in terms of computational cost. We have found that a grid of 150×150 points still does not eliminate the problem if filtering is not applied.[10] Numerical experiments showed that for this problem a 240×240 size grid is required. However, if a 150×150 grid is used with filtering, then all of the numerical